

Rapid Formation of Super-Earths around M Dwarf Stars

Alan P. Boss

*Department of Terrestrial Magnetism, Carnegie Institution of Washington, 5241 Broad
Branch Road, NW, Washington, DC 20015-1305*

boss@dtm.ciw.edu

ABSTRACT

While the recent microlensing discoveries of super-Earths orbiting two M dwarf stars have been taken as support for the core accretion mechanism of giant planet formation, we show here that these planets could also have been formed by the competing mechanism of disk instability, coupled with photoevaporative loss of their gaseous envelopes by a strong external source of UV radiation, i.e., an O star. M dwarfs that form in regions of future high-mass star formation would then be expected to have super-Earths orbiting at distances of several AU and beyond, while those that form in regions of low-mass star formation would be expected to have gas giants at those distances. Given that most stars are born in the former rather than in the latter regions, M dwarfs should have significantly more super-Earths than gas giants, as seems to be indicated by the microlensing surveys.

Subject headings: stars: planetary systems – stars: low-mass, brown dwarfs

1. Introduction

Microlensing surveys have discovered recently two “super-Earths” orbiting M dwarf stars, planets with masses of $\sim 5.5M_{\oplus}$ (Beaulieu et al. 2006) and $\sim 13M_{\oplus}$ (Gould et al. 2006). As microlensing detections yield only the ratio of the lensing planet mass to the lensing star mass, these planetary mass estimates rely heavily on the unproven assumption that the lensing star is an M dwarf. The super-Earths have been interpreted as being “failed cores” produced by the first step of the core accretion mechanism for gas giant planet formation. The super-Earths presumably failed to become gas giant planets because the growth of solid cores by collisional accumulation proceeds considerably slower at a fixed orbital radius around an M dwarf star than around a G dwarf star (Laughlin, Bodenheimer, & Adams 2004), and the disk gas is likely to have been dissipated in ~ 3 Myr, well before

such a core could accrete a significant gaseous envelope (Bally et al. 1998; Briceno et al. 2001; Haisch, Lada, & Lada 2001; Eisner & Carpenter 2003).

Microlensing surveys have also found evidence for two gas giant planets with masses of $\sim 1.5M_{Jup}$ orbiting M dwarfs (Bond et al. 2004; Udalski et al. 2005). Because the microlensing signal produced by gas giant planets is considerably stronger than that produced by super-Earths, these four detections suggest that given the limited signal-to-noise ratios of the ground-based photometry of microlensing events, super-Earths must be significantly more frequent companions to M dwarfs than gas giants. Thus these four detections have been taken as supportive of core accretion’s inability to form gas giants around low-mass stars (Beaulieu et al. 2006).

Radial velocity surveys were the first to discover the existence of gas giants and super-Earths around M dwarf stars. The M dwarf Gl 876 has an outer pair of gas giant planets as well as an inner super-Earth (Rivera et al. 2005). The M dwarfs Gl 436 and Gl 581 also appear to be orbited by super-Earths on short-period orbits (Butler et al. 2004; Bonfils et al. 2005). M dwarf planet surveys have only been underway for a few years, but they have already revealed that the frequency of close-in gas giants around M dwarfs appears to be lower than that around F, G, and K dwarfs (Endl et al. 2003, 2006). With time, these surveys will determine the frequency of longer period gas giants orbiting M dwarfs. Given the results to date of the radial velocity and microlensing surveys, however, there is a clear need to explain the formation of both gas giants and super-Earths around M dwarf stars.

We show here that disk instability can explain the formation of the gas giant planets orbiting M dwarfs found by both microlensing and radial velocity, as well as the super-Earths found by microlensing. We begin by presenting more details about a disk instability model (5CH) from Boss (2006a) that showed the possibility of forming gas giant protoplanets about M dwarfs, and then develop the reasoning behind the scenario for super-Earth formation by photoevaporation of gaseous protoplanets orbiting M dwarfs.

2. Numerical Methods and Initial Conditions

Model 5CH (Boss 2006a) was calculated with a finite volume code that solves the three dimensional equations of hydrodynamics and radiative transfer, as well as the Poisson equation for the gravitational potential. The code is second-order-accurate in both space and time (Boss & Myhill 1992) and has been used and discussed extensively in previous disk instability studies (e.g., Boss 2003, 2005, 2006a).

The equations are solved on a spherical coordinate grid with $N_r = 101$, $N_\theta = 23$ in

$\pi/2 \geq \theta \geq 0$, and $N_\phi = 512$. The radial grid extends from 4 AU to 20 AU with a uniform spacing of $\Delta r = 0.16$ AU. The θ grid is compressed toward the midplane in order to ensure adequate vertical resolution ($\Delta\theta = 0.3^\circ$ at the midplane). The ϕ grid is uniformly spaced to prevent any azimuthal bias. The central protostar wobbles in response to the growth of disk nonaxisymmetry, preserving the location of the center of mass of the star and disk system. The number of terms in the spherical harmonic expansion for the gravitational potential of the disk is $N_{Ylm} = 48$.

Model 5CH calculated the evolution of a $0.5M_\odot$ protostar surrounded by a protoplanetary disk with a mass of $0.065 M_\odot$ between 4 AU and 20 AU. The initial protoplanetary disk structure was based on an approximate vertical density distribution (Boss 1993). The initial disk temperatures were derived from the models of Boss (1995), with midplane temperatures of 300 K at 4 AU, decreasing monotonically outward to a distance of ~ 6.7 AU, where they were assumed to become uniform at an outer disk temperature of $T_o = 50$ K. The outer disk was then initially marginally gravitationally unstable in terms of the gravitational stability parameter Q , with an initial minimum value of $Q = 1.5$.

3. Gaseous Protoplanet Formation

Figures 1 and 2 show that model 5CH formed a number of clearly defined clumps after 215 years of disk evolution around a protostar with a mass of $0.5M_\odot$. The clumps grow inside spiral arms, which form in the innermost, marginally gravitationally unstable regions of the disk (~ 8 AU), because of the combination of relatively low Q and short orbital periods there (see Figure 1 of Boss 2006a). This is largely a result of the initial temperature profile assumed for the disk midplane (Boss 1995). Such a profile is to be expected for a protoplanetary disk in a region of low-mass star formation, or in any star-forming region prior to the formation of the first high-mass stars.

Table 1 lists the maximum densities in the four clumps evident in Figures 1 and 2, along with the clump masses M_c in units of the Jupiter mass M_{Jup} , the Jeans mass M_J at the average density and temperature of each clump, and the instantaneous values of the orbital semimajor axis and orbital eccentricity of each clump. In Figure 1, the first clump is located at 11 o'clock, the second at 3 o'clock, the third at 7 o'clock, and the fourth at 8 o'clock. Table 1 shows that each clump has a mass well in excess of the local Jeans mass, showing that these clumps are gravitationally bound. Their effective spherical radii are comparable to the critical tidal radii at their orbital distances, implying stability against tidal disruption by the protostar's tidal forces as well.

Because of the fixed nature of the numerical grid, the code is not able to provide the locally enhanced spatial resolution that these high density clumps require for their further evolution to be calculated correctly. While clump densities and lifetimes can be increased as the numerical spatial resolution is increased (Boss 2005), with a fixed grid code eventually the clumps are sheared apart. Meanwhile, new clumps continue to form and take their place. Calculations where the dense clumps are replaced by virtual protoplanets suggest that the protoplanets should be able to orbit stably for an indefinite period of time, even as the marginally gravitationally unstable disk continues to transport mass inward to the central protostar (Boss 2005). Similarly, SPH code calculations with a locally-defined smoothing length by Mayer et al. (2002) have shown that dense clumps should be able to survive their subsequent orbital evolution, though mergers, scatterings, and significant orbital evolution (both inward and outward) are to be expected when multiple clumps form, as in model 5CH.

While we cannot therefore predict the final outcome of model 5CH with any degree of certainty, the model suggests that one or more gas giant protoplanets with masses on the order of one to a few Jupiter masses could form by disk instability around an M dwarf star, with initial semimajor axes on the order of ~ 10 AU. In addition to mutual scattering events, Type II migration during the disk’s lifetime could force gas giants to migrate closer to their stars. It should be noted that model 5CH was not designed to attempt to form clumps *in situ* at the ~ 2.5 AU orbital separation at which the microlensing technique is most sensitive, but that with minor changes in the assumed initial disk profiles (i.e., a cooler inner disk), such an outcome would be likely.

4. Super-Earth Formation

If the M dwarf star and disk system represented by model 5CH had formed in a region of low-mass star formation like Taurus or Ophiuchus, the M dwarf would be expected to be accompanied by one or more $\sim 1M_{Jup}$ gas giant planets orbiting at distances of ~ 10 AU or less, possibly explaining the two gas giant planet microlensing detections (Bond et al. 2004; Udalski et al. 2005). However, most stars are formed in regions of high-mass star formation (Lada & Lada 2003), similar to the Orion and Eta Carina nebulae, where protoplanetary disks are subjected to a withering flux of FUV/EUV radiation from the nearby O stars (e.g., Bally et al. 1998). In the Eta Carina nebula, FUV/EUV fluxes are a factor of ~ 100 times higher than in Orion, yet protoplanetary disks are as commonplace in Carina as in Orion (Smith, Bally, & Morse 2003). Armitage (2000) found that the EUV flux alone in an Orion-like cluster was sufficient to photoevaporate gaseous disks within ~ 1 Myr around stars within 0.3 pc of the massive stars. In larger clusters like Eta Carina, similarly rapid

photoevaporation would occur for disks within 3 pc of the O stars.

Boss, Wetherill, & Haghighipour (2002) suggested that the Solar System was formed in a region of future high-mass star formation, such that after the massive stars formed, their FUV/EUV radiation was able to photoevaporate away not only the outer regions of the solar nebula, but also the gas envelopes of the two outermost gas giant protoplanets formed by disk instability (Boss 2003), stripping these two gaseous protoplanets down to rock/ice cores with only minor gaseous envelopes, i.e., turning them into the two ice giant planets, Uranus and Neptune.

One critical component of this scenario for ice giant planet formation is for the heavy elements to coagulate into dust grains and sediment down to the centers of the protoplanets faster than the protoplanets contract to planetary densities. Boss (1998) estimated that core formation in gaseous protoplanets would occur in $\sim 10^3$ yr, with a $1M_{Jup}$ protoplanet being able to form at most a $6M_{\oplus}$ rock/ice core. Helled, Kovetz, & Podolak (2006) performed a more detailed analysis, and confirmed that dust grains would settle down to form a central core in $\sim 10^3$ yr in a non-convecting protoplanet. When the effects of convective turbulence were included, the grains grew faster and reached the core in ~ 30 yr. Helled, Podolak, & Kovetz (2006) found that a $1M_{Jup}$ protoplanet requires $\sim 3 \times 10^5$ yr to contract from a radius of ~ 0.5 AU to ~ 0.1 AU. During this slow contraction phase, the protoplanet is able to accrete a significant number of km-sized planetesimals by gas drag capture in the protoplanet’s outer layers. These planetesimals will either be added to the solid core or will remain in the protoplanet’s envelope, but in either case the protoplanet will be highly enriched in heavy elements compared to the solar composition (Helled, Podolak, & Kovetz 2006). While much remains to be determined, it seems likely that gas giants with core masses and envelope enrichments similar to those of Jupiter and Saturn (Saumon & Guillot 2004) can be formed by disk instability.

The key factor for whether a gaseous protoplanet becomes a gas giant or an ice giant is the critical orbital radius r_e outside of which photoevaporation can remove the disk gas, and hence the protoplanetary envelope gas. A gravitational radius r_g can be defined to be the orbital radius where the sound speed of the UV-heated gas equals the gravitational escape speed from the protostar

$$r_g \approx \frac{GM_p}{c_s^2},$$

where M_p is the protostar mass and $c_s \approx 10$ km s⁻¹ for gas heated by EUV radiation and $c_s \approx 3$ km s⁻¹ for FUV radiation. Depending on the details of the photoevaporation model, r_e is expected to be smaller than r_g , with $r_e \sim 0.5r_g$ (Johnstone et al. 1998) or even smaller

(Adams et al. 2004). With $r_e \sim 0.5r_g$, for a G dwarf star like the Sun, $r_e \sim 50$ AU for FUV radiation and $r_e \sim 5$ AU for EUV radiation. Adams et al. (2004) argue that these values of r_e could be smaller by factors of as large as 5, i.e., to as small as ~ 10 AU to ~ 1 AU for FUV and EUV, respectively. While the exact value of r_e for any protostar will depend on the relative amounts of FUV and EUV received, we can calibrate r_e by noting that if photoevaporation was involved in the formation of the Solar System’s giant planets (Boss et al. 2002), then evidently $r_e < 9$ AU, in order to result in Saturn’s bulk composition (assuming little orbital migration of Saturn after its formation at ~ 9 AU).

These critical orbital radii depend linearly on the mass of the protostar. For an M dwarf star with 1/3 the mass of the Sun, r_e would then be expected to be ~ 3 AU or less, assuming the M dwarf protostar was exposed to the same FUV/EUV environment as the solar nebula. Gaseous protoplanets orbiting at this distance or beyond would lose the bulk of their hydrogen gas by photoevaporation, leaving a protoplanet composed primarily of the residual heavy elements (helium gas would also be lost by entrainment in the photoevaporative hydrogen flow). As a result, the final planet would be composed almost exclusively of the core and envelope heavy elements. The models of Helled, Podolak, & Kovetz (2006) suggest that a $\sim 1M_{Jup}$ protoplanet formed by disk instability could accrete as much as $\sim 30M_{\oplus}$ of km-sized planetesimals from the protoplanet’s feeding zone, using the same assumptions as are used in core accretion models (e.g., Pollack et al. 1996). Planetesimal scattering was neglected in these models, so this estimate appears to be a rough upper bound. [Cometesimal scattering by the giant planets is thought to be the source of the Oort Cloud comets and of the scattered disk component of the Kuiper Belt.]

Model 5CH produced several $\sim 1M_{Jup}$ gaseous protoplanets orbiting an M dwarf at ~ 10 AU. If this system formed in a region of future intense FUV/EUV radiation, these protoplanets would be stripped down to cores composed of heavy elements, with masses no larger than $\sim 30M_{\oplus}$. Assuming that mutual scattering and/or Type II migration had resulted in one of these planets ending up on a ~ 2.5 AU orbit, it could then be detected as a super-Earth by microlensing surveys.

5. Conclusions

Boss (2006b) pointed out that if the Orion-Carina scenario of Boss et al. (2002) was responsible for the formation of the Solar System’s ice giant planets, then a possible test of this combination of disk instability and photoevaporative losses would be to see if the dividing line (r_e) between gas giants and ice giants depends on the stellar mass: for lower mass stars, this critical radius should decrease proportionately. It remains for this prediction

to be tested by future extrasolar planet searches.

Because most M dwarf stars are expected to have been subjected to a high FUV/EUV radiation environment (Lada & Lada 2003), most M dwarf planets found by microlensing surveys would be expected to be super-Earths rather than gas giants, as seems to be the case so far, albeit based on a small sample of only four detections to date. Future microlensing detections will be important to determine if this provisional interpretation is correct.

The lower frequency of gas giant planets on short-period orbits around M dwarfs compared to F, G, and K dwarfs (Endl et al. 2003, 2006) may be a result of faster inward orbital migration around the more massive dwarfs. The well-known correlation of the presence of gas giants with the metallicity of the host star appears to be strongest for short-period planets (Sozzetti 2004), consistent with the expectation that Type II inward migration will be faster in metal-rich disks (Livio & Pringle 2003) and could thus result in a higher frequency of short-period gas giants (Boss 2005). The rate of Type II migration depends on the disk’s kinematic viscosity ν , and in standard viscous accretion disk theory (e.g., Ruden & Pollack 1991) $\nu = \alpha c_s h$, where α is a free parameter, c_s is the sound speed, and h is the disk thickness. M dwarfs will have cooler disks than G dwarfs (Boss 1995) because of their shallower gravitational potential wells and their (presumed) proportionately lower disk masses and hence smaller optical depths. As a result, M dwarf disks should be thinner and have smaller sound speeds than G dwarf disks, leading to smaller values of ν and hence longer Type II migration times. M dwarf planets should thus be less likely to undergo significant Type II migration prior to removal of their disk gas.

There is still an important role to play for the first step of the core accretion process in forming planets around M dwarfs. One of the short-period super-Earths found by the radial velocity surveys of M dwarfs (Gl 876 – Rivera et al. 2005) is known to be accompanied by two outer gas giant planets, implying that the super-Earth formed interior to the gas giants. The scenario presented in this paper would not be able to explain the formation of the Gl 876 system, unless the planets were able to interchange their radial ordering, which seems unlikely. Hence the Gl 876 super-Earth is likely to have been formed interior to its gas giants by the same collisional accumulation process that led to the formation of the terrestrial planets in our Solar System (e.g., Wetherill 1996). Taken as a whole, M dwarfs thus appear to present strong evidence for the formation of the same three classes of planets found in our Solar System: inner terrestrial planets formed by collisional accumulation, and outer gas giants or rock/ice giants (super-Earths) formed by disk instability, either in the absence of, or in the presence of, strong fluxes of FUV/EUV radiation, respectively.

I thank Michael Endl for discussions about M dwarf planets, the referee for several improvements to the manuscript, and Sandy Keiser for her computer systems expertise.

This research was supported in part by NASA Planetary Geology and Geophysics grant NNG05GH30G and by NASA Astrobiology Institute grant NCC2-1056. The calculations were performed on the Carnegie Alpha Cluster, the purchase of which was partially supported by NSF Major Research Instrumentation grant MRI-9976645.

REFERENCES

- Adams, F. C., et al. 2004, *ApJ*, 611, 360
- Armitage, P. J. 2000, *A&A*, 362, 968
- Bally, J., et al. 1998, *AJ*, 116, 854
- Beaulieu, J.-P., et al. 2006, *Nature*, 439, 437
- Bond, I. A., et al. 2004, *ApJ*, 606, L155
- Bonfils, X., et al. 2005, *A&A*, 443, L15
- Boss, A. P. 1993, *ApJ*, 417, 351
- . 1995, *Science*, 267, 360
- . 1998, *ApJ*, 503, 923
- . 2003, *ApJ*, 599, 577
- . 2005, *ApJ*, 629, 535
- . 2006a, *ApJ*, in press (20 May 2006 issue)
- . 2006b, in *Planet Formation 2004: Observations, Experiments, and Theory*, H. Klahr & W. Brandner, eds., Cambridge: Cambridge University Press, in press
- Boss, A. P., & Myhill, E. A. 1992, *ApJS*, 83, 311
- Boss, A. P., Wetherill, G. W., & Haghighipour, N. 2002, *Icarus*, 156, 291
- Briceño, C., et al. 2001, *Science*, 291, 93
- Butler, R. P., et al. 2004, *ApJ*, 617, 580
- Eisner, J. A., & Carpenter, J. M. 2003, *ApJ*, 598, 1341
- Endl, M., et al. 2003, *AJ*, 126, 3099
- . 2006, *ApJ*, submitted
- Gould, A., et al. 2006, *ApJ*, submitted
- Haisch, K. E., Lada, E. A., & Lada, C. J. 2001, *ApJ*, 553, L153
- Helled, R., Kovetz, A., & Podolak, M. 2006, in preparation
- Helled, R., Podolak, M., & Kovetz, A. 2006, *Icarus*, submitted
- Johnstone, D., Hollenbach, D., & Bally, J. 1998, *ApJ*, 499, 758
- Lada, C. J., & Lada, E. A. 2003, *ARAA*, 41, 57
- Laughlin, G., Bodenheimer, P., & Adams, F. C. 2004, *ApJ*, 612, L73

- Livio, M., & Pringle, J. E. 2003, MNRAS, 346, L42
Mayer, L., et al. 2002, Science, 298, 1756
Pollack, J. B., et al. 1996, Icarus, 124, 62
Rivera, E., et al. 2005, ApJ, 634, 625
Ruden, S. P., & Pollack, J. B. 1991, ApJ, 375, 740
Saumon, D., & Guillot, T. 2004, ApJ, 609, 1170
Smith, N., Bally, J., & Morse, J. A. 2003, ApJ, 587, L105
Sozzetti, A. 2004, MNRAS, 354, 1194
Udalski, A., et al. 2005, ApJ, 628, L109
Wetherill, G. W. 1996, Icarus, 119, 219

Table 1. Clump properties for model 5CH at 215 yr.

Clump	ρ_{max} (g cm ⁻³)	M_c/M_{Jup}	M_J/M_{Jup}	a (AU)	e
1	6.2×10^{-10}	1.0	0.74	8.7	0.040
2	2.7×10^{-9}	1.1	0.51	7.9	0.10
3	1.4×10^{-9}	1.3	0.57	9.0	0.093
4	1.6×10^{-9}	1.4	0.72	8.0	0.011

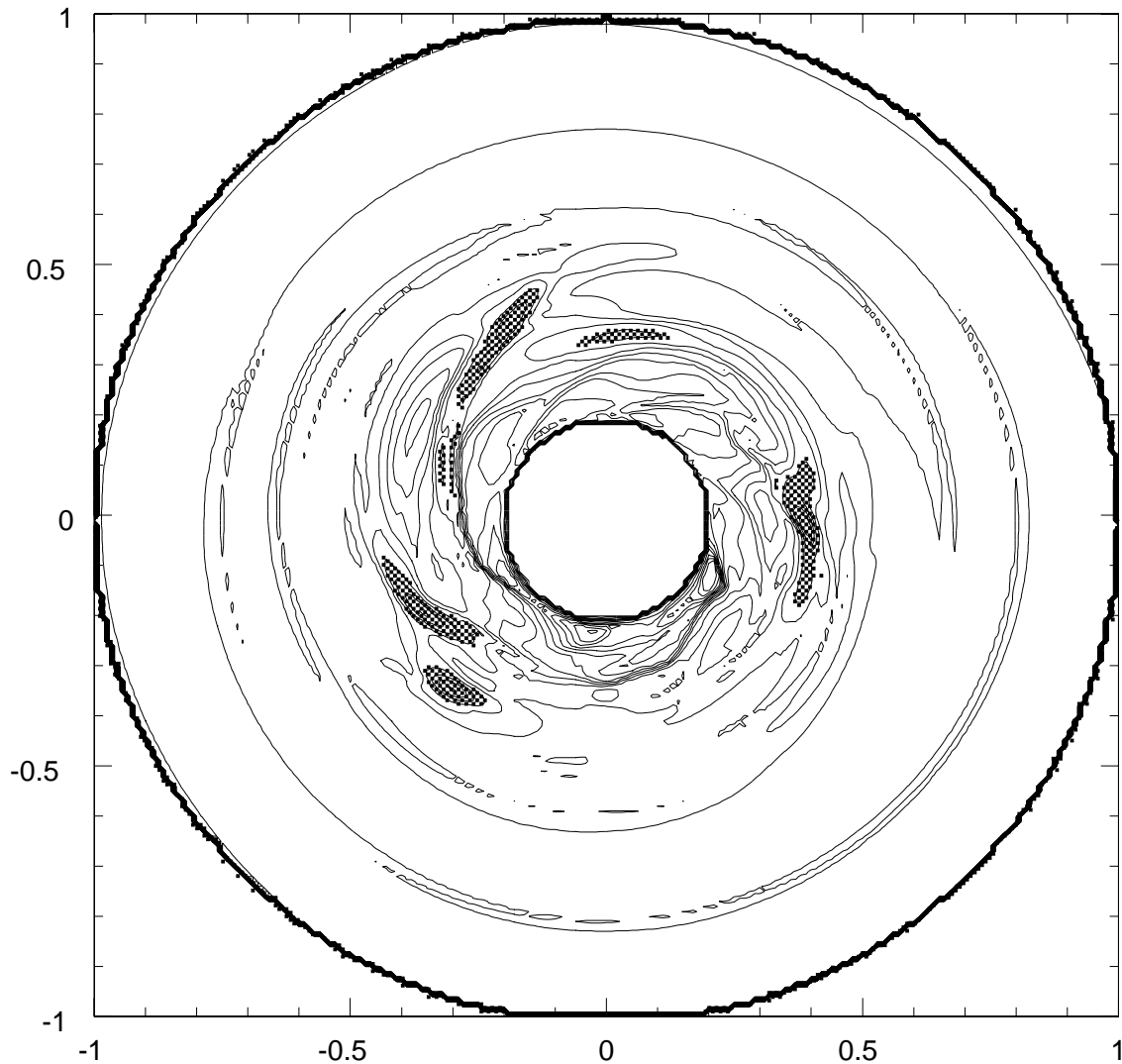


Fig. 1.— Equatorial density contours for model 5CH after 215 yrs of evolution. The entire disk is shown, with an outer radius of 20 AU and an inner radius of 4 AU, through which mass accretes onto the central protostar. Hashed regions denote spiral arms and clumps with densities higher than 10^{-10} g cm $^{-3}$. Density contours represent factors of two change in density. The four clumps described in Table 1 are numbered sequentially in counterclockwise order as they appear in this Figure, starting with clump #1 at 11 o'clock.

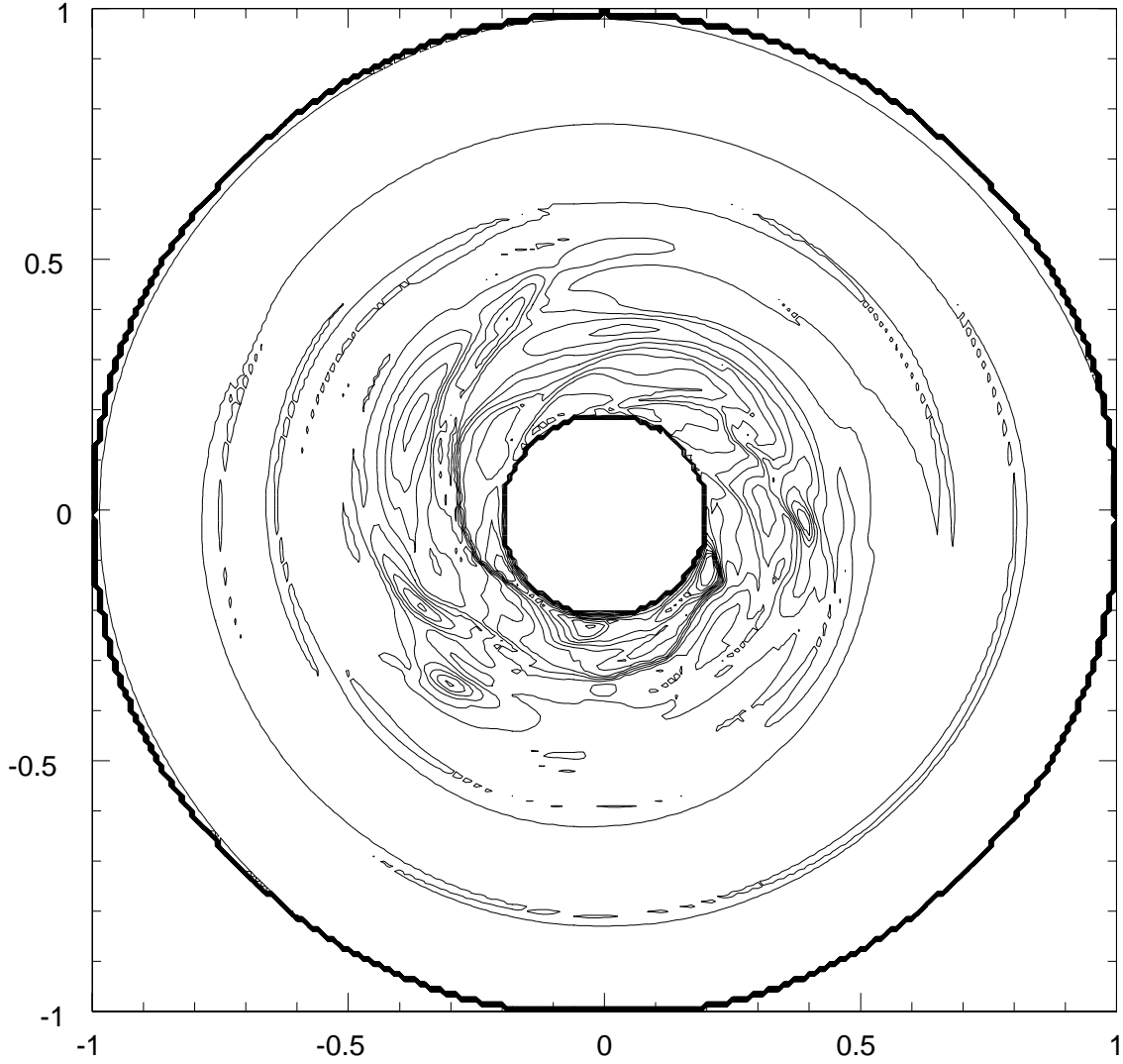


Fig. 2.— Same as Figure 1, but with cross-hatching removed to reveal the structure of the density contours in the densest regions.